Thermochimica Acta, 164 (1990) 153–160
Elsevier Science Publishers B.V., Amsterdam

THE NON-ISOTHERMAL REACTION KINETICS OF PYRITE WITH WATER VAPOUR

IAN C. HOARE * and JOHN H. LEVY

CSIRO, Division of Fuel Technology, Lucas Heights Research Laboratories, Private Mail Bag 7, Menai, NSW 2234 (Australia)

(Received 20 November 1989)

ABSTRACT

The reaction of pyrite with water vapour, at pressures ranging from 10 to 80 kPa, has been studied under non-isothermal conditions. Numerical methods were used to abstract kinetic parameters from the differential rate equations representing kinetic models of the thermogravimetric (TG) data. The first and major stage of mass loss proceeds by reaction of water with pyrite to form a porous layer of pyrrhotite around a contracting pyrite core. A topochemically controlled, contracting volume reaction model gives an excellent fit to the TG data and is confirmed by microscopic studies. The second stage consists of oxidation of the pyrrhotite to magnetite and is best described by a reaction model based on three-dimensional diffusion control.

INTRODUCTION

Levy and White [1] have recently examined the reaction of pyrite and water vapour as part of a program to investigate the reactions of minerals commonly present in Australian Tertiary oil shales. This paper extends this work by analysing the non-isothermal reaction kinetics of pyrite in water vapour using techniques developed and successfully applied [2] to the decomposition of pyrite in nitrogen.

For a solid undergoing a reaction under isothermal conditions the rate is given by

$$-\mathrm{d}\phi/\mathrm{d}t = kg(\phi) \tag{1}$$

where ϕ is the fraction of unreacted solid and $g(\phi)$ is a function appropriate to the reaction mechanism. For a solid heated at a constant rate, $\mathrm{d}T/\mathrm{d}t = \beta$, it is common practice to combine the isothermal equation with the Arrhenius expression, $k = A\mathrm{e}^{-E/RT}$, and the linear heating rate, β, to give the non-isothermal kinetic equation

$$\mathrm{d}\phi/\mathrm{d}T = (A/\beta)g(\phi)\ \mathrm{e}^{(-E/RT)} \tag{2}$$

* Author to whom correspondence should be addressed.

0040-6031/90/$03.50

which on integration gives

$$G(\phi) = \int d\phi/g(\phi) = -(A/\beta)\int e^{(-E/RT)}dT \quad (3)$$

In previous papers [2–5] we have detailed the way in which the kinetic parameters, A and E, can be obtained from the rate expression using predictor–corrector numerical methods, along with the choice of the appropriate kinetic model function, $g(\phi)$. Briefly, software packages were devised to allow the direct solution of the non-isothermal rate equations using the Gear method [6] coupled with high-speed graphical display to compare experimental and calculated TG and DTG curves to assess the various kinetic models. Initial estimates of the kinetic parameters obtained in this way were then refined iteratively by non-linear regression.

EXPERIMENTAL

A Cahn RG thermobalance equipped with a sample enclosure allowing reactions in water vapour/gas atmospheres, as described previously [1], was used to obtain thermogravimetric (TG) data. Ground and sieved samples (63–125 μm) were used to minimise the effects of differing particle size distributions on the TG curves. Approximately 10 mg was spread thinly on the bottom of the pan and heated at 10 °C min^{-1} in nitrogen flowing at 130 ml min^{-1} for a series of water vapour partial pressures ranging from 10 to 80 kPa. In each case there was a stoichiometric excess of water vapour. Experimental TG and DTG data were transferred to an IBM 4381 mainframe computer which was used for kinetic analysis, using the software packages described above.

RESULTS AND DISCUSSION

The reaction of pyrite with water vapour proceeds [1] via the two clearly defined stages shown in Fig. 1, to produce magnetite as the final product from the intermediate, hexagonal pyrrhotite. The first stage of mass loss is described by the reactions

$$36FeS_2 + 22H_2O \rightarrow 3Fe_{12}S_{13} + 11SO_2 + 22H_2S \quad (4)$$

and

$$SO_2 + 2H_2S \rightarrow 3S + 2H_2O \quad (5)$$

whereas the second, considerably less rapid stage has a mass loss given by

$$Fe_{12}S_{13} + 16H_2O \rightarrow 4Fe_3O_4 + 13H_2S + 3H_2 \quad (6)$$

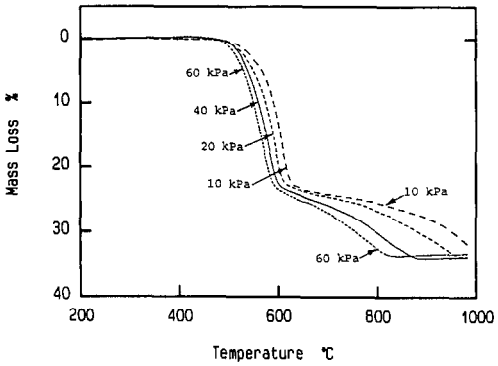

Fig. 1. Thermogravimetric curves for the reaction of pyrite heated at 10 °C min^{-1} in different water vapour pressures in nitrogen.

For the first stage of the reaction, optical microscopy clearly showed [1] that the development and geometry of the reaction is very similar to that found for the thermal decomposition of pyrite in nitrogen [2]. During the progress of the first stage reaction in single particles of pyrite, a layer of pyrrhotite is produced around a core of unreacted pyrite, with the reaction interface advancing inwards in three dimensions. Secondary scanning electron microscopy also showed a high degree of open porosity in the pyrrhotite product with similar structural features to those found previously [2]. No unreacted pyrite remained at the end of the first stage and the principal product was hexagonal pyrrhotite. The second, much slower, stage of the reaction is the oxidation of the pyrrhotite by water vapour to form magnetite. Microprobe analysis on single particles showed a gradual loss of sulphur throughout this second stage until none remained at the conclusion

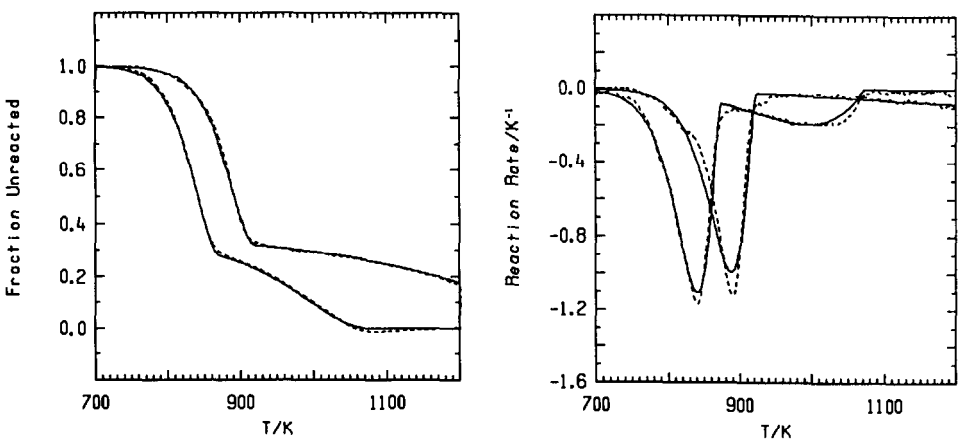

Fig. 2. Example fits of the kinetic models to the TG data obtained at 80 and 10 kPa water vapour pressure.

of the reaction. This loss was spread evenly across the particle so that there was no reaction interface apparent for this stage. This is in accord with results from optical and scanning electron microscopy [1].

In view of the marked similarities between the first stage of the reaction of pyrite with water vapour and for that of the thermal decomposition of pyrite, it is not surprising that the same kinetic model proved the most satisfactory. Figure 2 shows that a model based on a three-dimensional shrinking core with chemical rate control gives an excellent fit to the experimental data of the first stage. If the rate of product formation is determined by the rate of chemical reaction at the advancing interface and the interface advances in three dimensions, then the non-isothermal rate is [7]

$$-\mathrm{d}\phi/\mathrm{d}T = (A/\beta)g(\phi_1)\,\mathrm{e}^{(-E/RT)} \tag{7}$$

where

$$g(\phi_1) = \phi^{2/3} \tag{8}$$

The second stage of the reaction exhibited a very shallow TG curve, with an inherently very broad DTG curve. The use of a three-dimensional diffusion-controlled kinetic model was required to model this stage. Both the Jander [8] and the Ginstling–Brounshtein [9] equations provided a satisfactory fit to the experimental data for this stage. Other kinetic models, with the various forms of $g(\phi)$ listed by Brown et al. [7], did not fit as well.

If the overall rate is determined by diffusion of species across an increasing barrier of product, then the rate [8] is given by

$$-\mathrm{d}\phi/\mathrm{d}T = (A/\beta)g(\phi)_2\,\mathrm{e}^{-E/RT} \tag{9}$$

where

$$g(\phi)_2 = \phi^{1/3}(\phi^{-1/3} - 1)^{-1} \tag{10}$$

or alternatively [9] by

$$g(\phi)_2 = 3/2(\phi^{1/3} - 1)^{-1} \tag{11}$$

Therefore, the complete TG or DTG curve for the reaction kinetics of a single pyrite particle is well described by

$$\mathrm{d}\phi/\mathrm{d}T = (A_1/\beta)g(\phi)_1\,\mathrm{e}^{-E_1/RT} + (A_2/\beta)g(\phi)_2\,\mathrm{e}^{-E_2/RT} \tag{12}$$

Figure 2 shows that the calculated TG and DTG curves derived from eqn. (12) are in excellent agreement with the experimental curves.

Although the 3-D diffusion-controlled kinetic model provides the best description of the second-stage experimental kinetic data, it is difficult to provide further evidence to support this model. Examination of single particles taken at various stages of reaction in the second stage have the same open porous, uniform structure as found previously [2]. Microprobe

analysis revealed no concentration gradients or advancing interface across the single particles which suggests that the rate-controlling step is either solid-state diffusion of hydrogen sulphide from the pore walls, or the diffusion of water into the radially elongated pyrrhotite particles.

The effect of pressure

The effect of varying water vapour pressure is indicated in Fig. 1 where the complete TG and DTG curves move up the temperature axis as the pressure decreases. The pressure effect on the first stage is small and an examination of the kinetic parameters given in Table 1 shows that both A_1 and E_1 remain relatively constant over the pressure ranged studied. There is a slight decrease in activation energy with increasing pressure which can be described by the logarithmic relationship of Fig. 3. When the rate of product formation is determined by the rate of chemical reaction at the advancing interface there should be no pressure dependence on the activation energy. The slight trend observed is probably due to experimental factors but could arise from a small contribution from another mechanism with a diffusion-controlled rate.

In contrast, the effect of pressure on the second stage is quite marked which provides additional support to the model of three-dimensional diffusion control for the second stage mechanism. The values of A_2 and E_2 increase considerably with increasing pressure as shown in Table 1 where the activation energy has increased by about 60 kJ mol^{-1} over the pressure range and the pre-exponential constant by some five orders of magnitude. It was possible to fit the variation of E_2 with pressure, by non-linear least-squares, to an exponential function

$$E_2 = 100.0(2.04 - 1.00\ e^{(-0.1751P)}) \quad (13)$$

where E_2 is the activation energy and P is the pressure. This function, which is shown along with the experimental data in Fig. 3, suggests that as

TABLE 1

Kinetic parameters obtained at different water vapour pressures

Pressure (kPa)	A_1 (s^{-1})	E_1 (kJ mol^{-1})	A_2 (s^{-1})	E_2 (kJ mol^{-1})
10.0	5.5×10^9	204	5.8×10^1	121
15.0	5.6×10^9	202	3.0×10^2	128
20.0	5.6×10^9	200	1.7×10^3	134
30.0	5.6×10^9	199	2.7×10^3	139
40.0	5.9×10^9	198	5.4×10^4	158
60.0	5.9×10^9	195	4.1×10^5	168
80.0	6.3×10^9	194	5.7×10^6	182

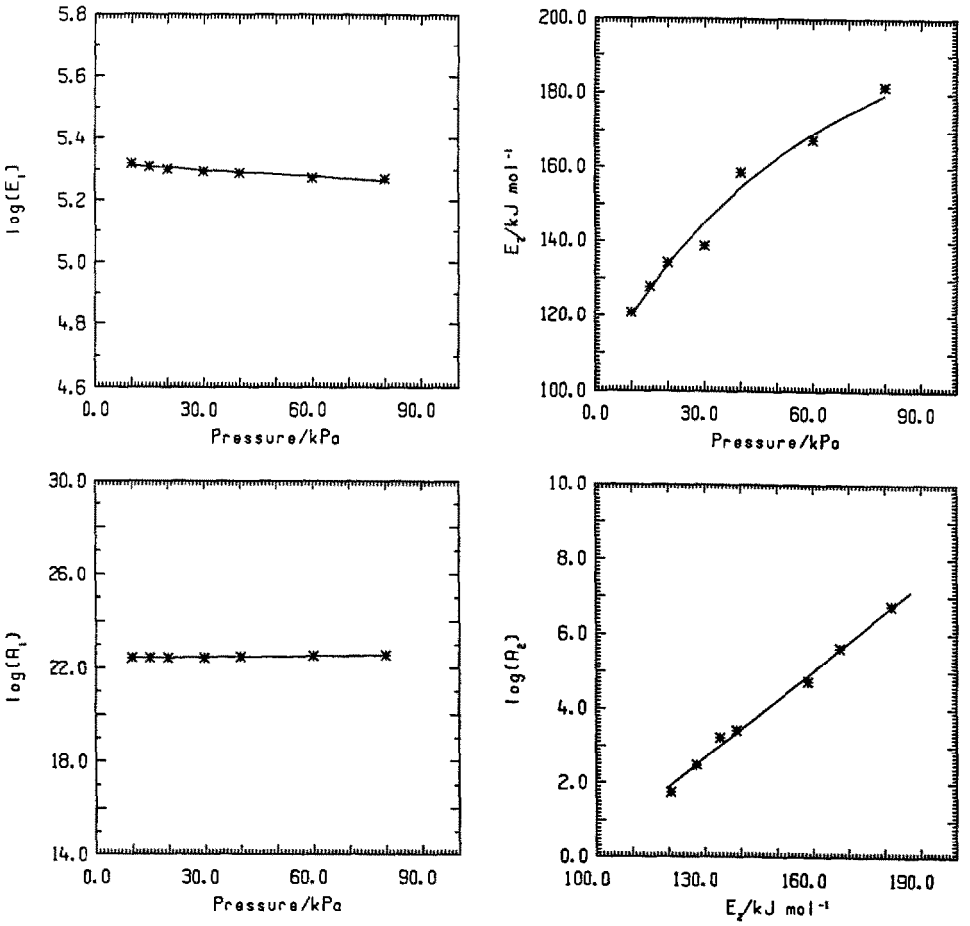

Fig. 3. Relationships between the calculated kinetic parameters and water vapour pressure, and the relationship of log A_2 and E_2 for the second reaction stage.

the pressure increases, the activation energy increases to a value around 200 kJ mol^{-1}, with a minimum value near to 100 kJ mol^{-1}. Although other workers [10,11] have found similar relationships in thermal decompositions, they also noted that the effects are quite complex and attempts to describe the pressure relationships in the rate equation have met with little success. The usual way [12] of describing the pressure relationship in the rate equation is with the pressure function, $1 - \exp(-\Delta G/RT)$, but this was unsuitable for the pressure effects observed in this work.

The kinetic compensation effect

Further examination of the pre-exponential factor and the activation energy for the second stage revealed a definite logarithmic relationship between A_2 and E_2, as illustrated in Fig. 3. This suggests the presence of a

kinetic compensation effect [12], a term frequently used when different pairs of pre-exponential constants and activation energies are obtained, either from the thermoanalytical curves of similar substances, from curves of the same substances recorded under different experimental circumstances as observed here, or from the same curve evaluated with different kinetic functions. The points belonging to the different A_i, E_i pairs fit a straight line in the log A versus E plane, i.e. the Arrhenius parameters are related by the equation

$$\log A = a + bE \tag{14}$$

where A and E are the frequency factor and activation energy respectively, and a and b are constants known as the compensation parameters. Galwey and Brown [13] have shown that mean compensation parameters for heterogeneous catalysis generally lie within the limits $16.6 < a < 19.0$ and $0.099 < b < 0.118$. The values, $a = -7.57$ and $b = 0.079$, obtained in this work, are substantially different from those of typical catalyst reactions, but quite similar to those found by Ball and Casson [10] for the thermal decomposition of lead carbonate and lead hydroxide carbonate. They also used a diffusion model to describe the decomposition kinetics.

There is a possible explanation for the observation of the kinetic compensation effect if the formation of intermediate stages between the products and reactants is considered. When a reaction interface is involved in the reaction rate, as is the case for a three-dimensional diffusion-controlled mechanism, and the intermediate stages, or complexes, all involve active sites, then it may be necessary to consider this as an additional restraint on the overall kinetics of the reaction. Should the total number of active sites be limited, a bottleneck effect may arise and the concentration of intermediates is no longer simply dependent on the reaction temperature and the Arrhenius parameters. In addition, the rate is now dependent on the proportion of active sites occupied by the intermediates involved in the rate-determining step. These intermediates and all others in equilibrium with the limited number of active sites will introduce a temperature dependence for the rate which is different to that of a reaction where there is no limitation on the number of active sites.

CONCLUSIONS

This work has further applied predictor–corrector numerical methods to the analysis of non-isothermal TG data to determine the nature of solid state reactions. The results have shown that the reaction of pyrite in water vapour can be described by a topochemically-controlled contracting core model for the first stage, followed by a three-dimensional diffusion-controlled model

for the second stage oxidation of pyrrhotite to magnetite. The models are supported by optical and electron microscopy results.

The effect of pressure is slight for the first stage of the reaction, but pronounced for the second stage, indicative of the two kinetic mechanisms controlling the overall reaction rate. For the second stage, increasing water vapour pressure resulted in significant increases in the Arrhenius parameters and although it was possible to establish an exponential relationship, a simple pressure function could not account for the observed variations in A and E with pressure. The kinetic compensation effect observed for the second reaction stage can be explained in terms of the three-dimensional diffusion model employed and the assumption that active sites at the reaction interface are limited in number.

ACKNOWLEDGEMENTS

We extend our thanks to Harry Hurst and Bill Stuart of CSIRO Division of Fuel Technology, to Tim White of ANSTO Materials Division and Prof. Slade Warne of the University of Newcastle for their helpful discussions. This work was partially funded by a CSIRO/University Collaborative Research Fund and a Collaborative Research Agreement with Esso Australia Ltd.

REFERENCES

1 J.H. Levy and T.J. White, Fuel, 67 (1988) 1336.
2 I.C. Hoare, H.J. Hurst, W.I. Stuart and T.J. White, J. Chem. Soc., Faraday Trans. I. 84 (1988) 3071.
3 I.C. Hoare and W.I. Stuart, Thermochim. Acta, 113 (1987) 53.
4 W.I. Stuart and J.H. Levy, Proc. 14th Conf. of the North American Thermal Analysis Society, San Francisco, 15–18 September 1985, pp. 297–301.
5 I.C. Hoare and W.I. Stuart, Proc. 15th Conf. of the North American Thermal Analysis Society, Cincinnati, 21–24 September 1986 pp. 267–272.
6 C.W. Gear, Numerical Initial Value Problems in Ordinary Differential Equations, Prentice–Hall, Englewood Cliffs, NJ, 1971.
7 W.E. Brown, D. Dollimore and A.K. Galwey, Comprehensive Chemical Kinetics, Vol. 22, Elsevier, Amsterdam, 1980.
8 W. Jander, Z. Anorg. Allg. Chem., 163 (1927) 1.
9 A.M. Ginstling and B.I. Brounshtein, Zh. Prikl. Khim. (Leningrad), 23 (1950) 1249.
10 M.C. Ball and M.J. Casson, J. Therm. Anal., 28 (1983) 371.
11 J.M. Criado, M. Gonzalez and M. Macias, Thermochim. Acta, 113 (1987) 39.
12 G. Pokol and G. Varhegyi, CRC Critical Reviews in Analytical Chemistry, 19 (1988) 65.
13 A.K. Galwey and M.E. Brown, J. Catal., 60 (1979) 335.